International Journal of Recent Technology and Engineering (IJRTE)
ISSN: 2277-3878 (Online), Volume-8 Issue-6, March 2020

Boundary Layer Control of Airfoil using Rotating Cylinder

Dharmendra P, Abhinav Verma, Chandana J P Reddy, Jitvan Suri S, Vishal M

Abstract**: *The requirement for improving the aerodynamic efficiency and delaying the formation of stall over the wing has been of prime importance within the field of aviation. The main objective of the project is to further improve upon these two parameters. The configuration used for analysis consists of a NACA 2412 airfoil of chord length 0.982m with a 64mm cylinder at the leading edge. Analysis is completed using ANSYS Fluent, with a freestream velocity of 10m/s. The aerodynamic characteristics of three configuration bare airfoil, Airfoil with static cylinder and Airfoil with rotating cylinder are tabulated and plotted. The comparison is then followed by pressure and velocity contours to visualize the flow over each configuration. The rotating cylinder configuration shows a improvement in the aerodynamics characteristics. The rotating cylinder configuration gives the most favourable result. This study has a potential application in high lift devices and can be used as stall delaying device.***

Keywords **: *Boundary Layer, Flow Separation, Magnus Effect, Rotating cylinder.***

I. INTRODUCTION

In the field of aerodynamics, it is important to know the flow behaviour over an airfoil surface. This can provide a path to style and use different techniques in improving the aerodynamic characteristics of an airfoil. The delay of boundary layer separation and also the improvement of the lift to drag ratio of an airfoil are always of great importance, not only to the look of the advanced aircrafts but also to the control of the boundary layer because the flow moves along the airfoil surface, it loses momentum and also the velocity values within the fluid layers along the perpendicular distance from the surface becomes zero, this continues down the airfoil until a degree where the flow cannot remain attached to the surface, this phenomenon is named as flow separation. The flow separation is related to the creation of vortices and reversed flows which contribute to a drastic call in the lift and a major increase within the drag force of the airfoil. A number of the methods to control this are blowing, suction, vortex generation and moving surfaces technique.

The Magnus effect is an observable phenomenon that's commonly related to a spinning object moving through the air or a fluid. The trail of the spinning object is deflected during a manner that's not present when the article isn't spinning. The deflection is explained by the difference in pressure of fluid on opposite sides of the spinning object. When a spinning body during a fluid flow creates a perpendicular force called the lift and an opposing force drag it's called the Magnus effect. These forces working on the cylinder provides further lift forces for the airplane. The amount of drag and lift is varied by adjusting the rotating speed of the body.

Magnus Effect

A spinning object moving through a fluid departs from its straight path due to pressure differences that develops within the fluid as a results of velocity changes induced by the spinning body.

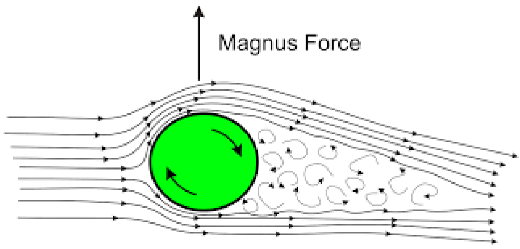

Fig 1. Flow over Rotating Cylinder

This force causes a deflection of the cylinder within the upwards direction. The deflections are often explained by the difference in pressure of fluid on opposite sides of the cylinder. When a cylinder body in a fluid creates a perpendicular force called the lift and an opposing force drag it's called the Magnus effect. These forces functioning on the cylinder provides a further lift forces for the airplane. The amounts of drag and lift are often varied by adjusting the rotating speed of the body.

Boundary Layer

As an object moves through a fluid, or as a fluid moves past an object, the molecules of the fluid near the article are disturbed and move round the object. Aerodynamic forces are generated between the fluid and also the object. The magnitude of those forces depend upon the form of the article, the speed of the article, the mass of the fluid going by the article and on two other important properties of the fluid; the viscosity and also the compressibility of the fluid.

Manuscript received on March 15, 2020.
Revised Manuscript received on March 24, 2020.
Manuscript published on March 30, 2020.
* Correspondence Author

Dharmendra P*, Assistant Professor, Dayananda Sagar College of Engineering, Bangalore, India. Email: daponnaswami07@gmail.coms

Abhinav Verma, Dept. of Aeronautical Engineering, Dayananda Sagar College of Engineering, Bangalore, India. Email: abhinave1997@gmail.com

Chandana JP Reddy, Dept. of Aeronautical Engineering, Dayananda Sagar College of Engineering, Bangalore, India. Email: desertstrom25@gmail.com

Jitvan Suri S, Dept. of Aeronautical Engineering, Dayananda Sagar College of Engineering, Bangalore, India. Email: suri.s.jitvan@gmail.com

Vishal M, Dept. of Aeronautical Engineering, Dayananda Sagar College of Engineering, Bangalore, India. Email: vishal1641998@live.com.

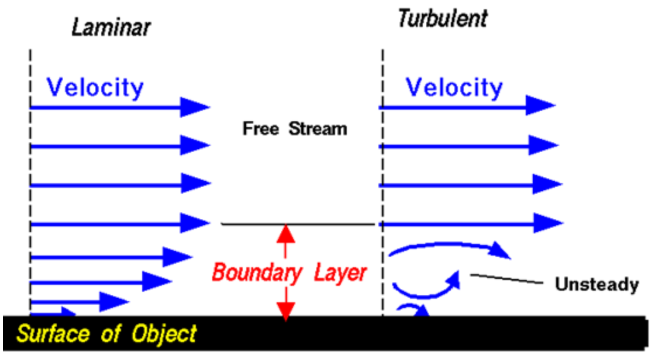

Fig 2. Boundary Layer formation over an object

As the fluid moves past the object, the molecules right next to the surface stick on with the surface. The molecules just above the surface are stalled in their collisions with the molecules sticking to the surface. These molecules successively block down the flow just above them. The farther one moves, it is removed from the surface, the less the collisions suffering from the object surface. This creates a skinny layer of fluid near the surface during which the speed changes from zero at the surface to the free stream value removed from the surface.

Flow Separation

Flow separation is the detachment of a boundary layer from a surface into a wake. Separation occurs in flow that's slowing down, with pressure increasing, after passing the thickest part of a streamline body or passing through a widening passage, for instance, flow against an increasing pressure is understood as flow in an adverse pressure gradient. The flow gets separated when it has travelled far enough in an adverse pressure gradient that the speed of the flow relative to the surface has stopped and reversed the direction. The flow becomes detached from the surface, and instead takes the kinds of eddies and vortices. Much effort and research has gone into the look of aerodynamic surface contours and added features which delay flow separation and keep the flow attached for as long possible.

Fig 3. Flow Separation over an airfoil

When the boundary layer separates, its displacement thickness increases sharply, which modifies the outside potential flow and pressure field.

In this project we are employing a cambered airfoil NACA 2412. And the analysis is carried out in ANSYS Fluent CFD. All the CAD drawings are made in Design modeller of the ANSYS Fluent workbench for the computability and accuracy.

A. Scope of the work

- Better understanding of the effect of Boundary Layer and interaction with the airfoil body.
- Using the obtained 2D data to model and analyse 3D structure and study on it.
- Design various cylinder configurations to optimize the Lift and Drag.
- Finding suitable CFD model to improve the accuracy of the results.

B. Objective

- To delay boundary layer separation towards the trailing edge of the airfoil.
- To improve the quality of flow over the airfoil.
- To reduce the exponential increase in Drag at higher angles of attack.

II. DESIGN METHODOLOGY

A. Formulation/ Theoretical Background

The main physical phenomena that is employed in this project is Magnus Effect. The flow around the airfoil is improved by using a rotating cylinder at the leading edge of the airfoil. A lift force is generated due to this, thereby increasing efficiency.

The Reynolds number for the analysis was calculated using the below formula,

$$Re = \rho u L/\mu$$

Where

ρ = Density (kg/m3) = 1.225 kg/m^3

μ=Dynamic viscosity = 1.7894*10^{-5}kg/m*s

L = Length (m) = 0.982 m

u = Flow speed (m/s) =10 m/s

On the substituting the values of the above terms, we get the Re of about 675000 which is a turbulent flow. Boundary layer equations like Navier-Stokes equation for Turbulent flow and incompressible flow were utilized for determining the effect of boundary layer on the surface of airfoil due to the rotating cylinder. Spalart Allmaras CFD flow model is used to obtain good boundary layer interactions and was found suitable for this project.

The ratio of cylinder rotational speed to freestream velocity is $Uc/U\infty$. The ratio was varied between 1 to 4 times the freestream velocity to find the optimal performance of the cylinder.

Lift and Drag values were theoretically calculated using the following formula

$$Lift = 0.5*\rho\infty*V\infty*V\infty*S*C_L$$

$$Drag = 0.5*\rho\infty* V\infty*V\infty*S*C_D$$

Where

$\rho\infty$ = Density of air = 1.225 kg/m^3

S = Area = 1m^2 (2D)

$V\infty$ = Freestream velocity = 10m/s

B. Design of the Model

NACA 2412 coordinate files were imported using Airfoil Tools into ANSYS Design Modeller. The geometry was designed as shown in the figure.

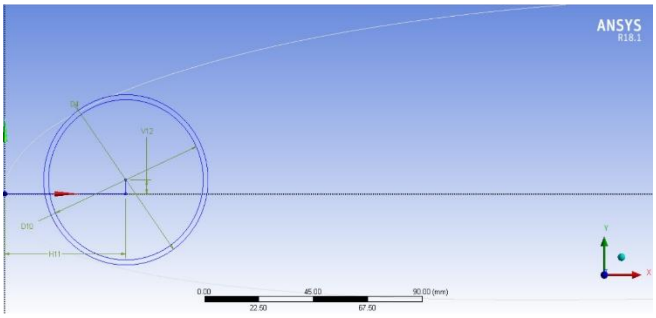

Fig 4. Cut-out cylinder geometry

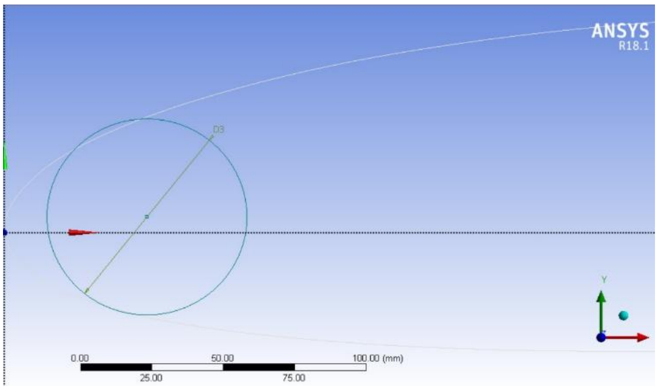

Fig 5. Rotating cylinder geometry sketch

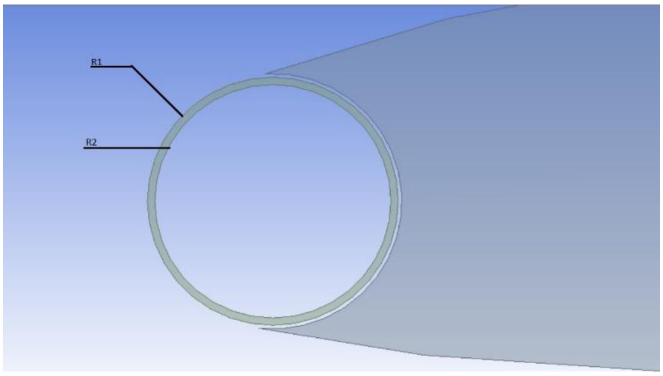

Fig 6. Rotating cylinder geometry dimensions

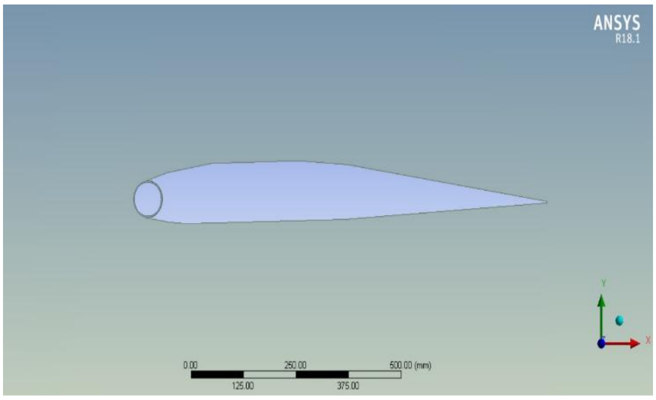

Fig 7. Final geometry

TABLE 1. GEOMETRICAL DIMENSIONS

Parameter	Dimensions (mm)
Cut-out cylinder(Diameter)	70
Fluid cylinder(Diameter) (R1)	68
Rotating cylinder(Diameter) (R2)	64
Horizontal distance from leading edge	50
Vertical distance from chord line	5.6
Chord length	982

C. Meshing

The mesh was generated using All Triangles method with body sizing to make the domain mesh finer. Edge sizing on the airfoil and the cylinder were used to capture the profile perfectly and to obtain accurate solutions. Connections were provided to the outer fluid domain and inner fluid domain to make the mesh into a single component.

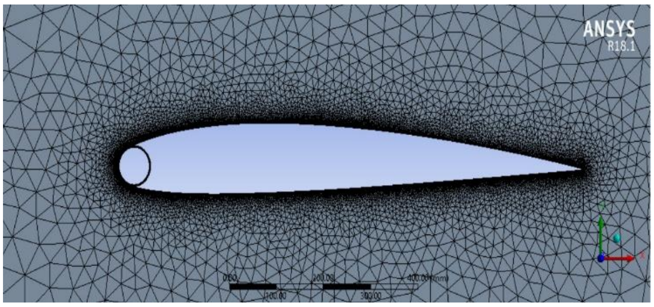

Fig 8. Mesh around the Airfoil

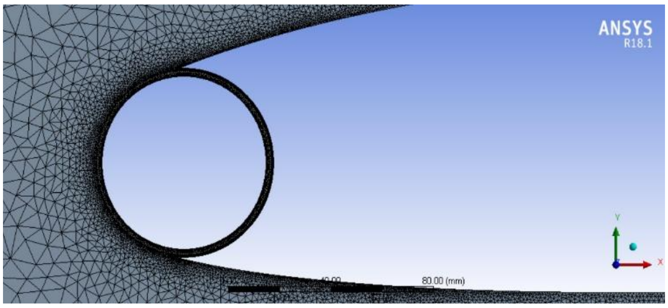

Fig 9. Mesh around the Cylinder

The domain size is 6 times the chord length(c) from the leading edge, 6c from the chord line to the far field, 16c at the outlet from the leading edge which makes sure that there are no far field interactions. Number of nodes is about 65,300 and number of elements is about 113000.

D. Mesh Independency Test

The way to check if the solution is independent of grid or not to create a grid with more cells to compare the solutions of the two models. By refining the grid and checking for drag coefficient we find that for about 110000 cells the values don't vary substantially affecting the output. This is chosen to improve the accuracy and reduce the computation time.

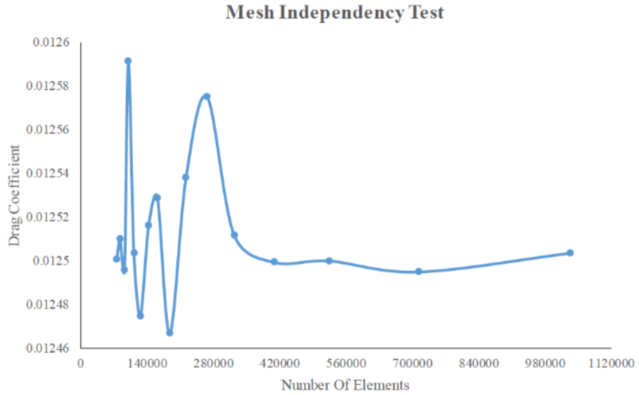

Fig 10. Mesh Independency test for rotating cylinder

E. Validation of the software

First step in checking the software is by comparing the results obtain to the results published by the research papers that we are using for reference. The error between the results obtained and the research papers should be the within 10% tolerance. This ensures that results obtained by the software and the methodology is accurate and reliable for the project. The following table gives the insight of the validation that was performed on the NACA 2412 airfoil.

TABLE II. VALIDATION DATA

Angle of Attack	CL(Reference)	CL(obtained)	Error %
0°	0.204	0.204	0
2°	0.416	0.403	3.12
4°	0.625	0.592	5.28
6°	0.824	0.757	8.13
8°	0.972	0.887	8.74
10°	1.157	1.051	9.16
12°	1.201	1.103	8.15
14°	1.255	1.039	15.1
16°	1.191	1.093	8.22

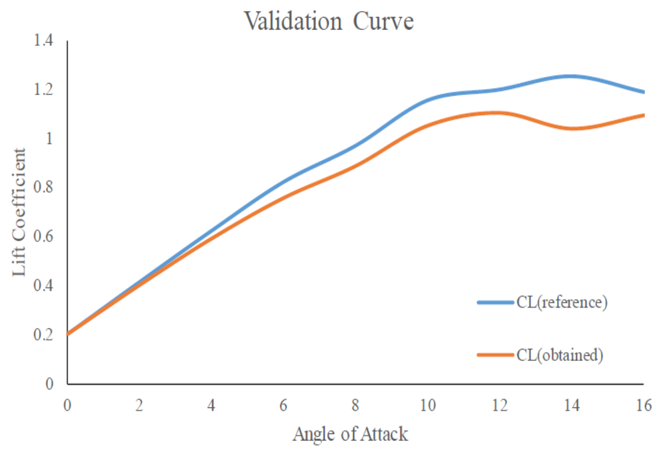

Fig 11. Validation Curve

F. Setup/ Analysis

Spalart Allmaras Turbulence model was used with mesh motion in cell zone conditions. Inlet velocity of 10m/s was given for the analysis. The cylinder rotation was varied to optimal value of about 11000rpm (3.7 times the freestream velocity) in the clockwise direction. The step size was 0.0001 to obtain solution with maximum accuracy. Lift and Drag coefficient were plotted at the airfoil and the cylinder location. The convergence condition was set to 0.0001 to maximize the accuracy of the solution obtained. The reference values were computed from inlet and hybrid initialization was used. Solution animation was used to study the flow behaviour around the geometry. A internal connection was given to outer fluid domain and inner fluid domain to make them as a single unit.

G. Optimising the cylinder location and size

Cylinder with 109mm at 0.2c was initially designed but this configuration had very high drag. In the second iteration 44mm cylinder at 0.025c was analysed. But this configuration didn't provide adequate lift as per the requirement and hence was discarded. The final configuration that we affixed on was 64mm cylinder at 0.050c of the chord length which had favourable aerodynamic characteristics.

III. RESULTS AND DISCUSSIONS

The lift, drag, and efficiency values of each of the configuration (bare airfoil, airfoil with static cylinder, airfoil with rotating cylinder) was tabulated at various angles of attack. The following table gives the comparison between them. Table III shows that the least performing configuration is the one with static cylinder. This is due to the fact that the cylinder produces a lot of drag. As the cylinder starts to rotate we observe that the performance increases. At low angles of attack the efficiency of this configuration is much higher than the bare airfoil configuration. We also observe an increase in lift coefficient with the rotating cylinder. The cylinder provides an additional lift to the airfoil. The part of flow from the pressure surface gets redirected to the suction surface due to the spinning motion of the cylinder thereby energizing the boundary layer on the suction surface.

The corresponding graphs of angle of attack versus respective aerodynamic characteristics is shown in the figures below.

The bare airfoil and the rotating cylinder configuration gives the best results as observed from the graph.

The C_L distribution of the three configurations remain the same but the C_L of the static cylinder starts dropping as the angle of attack is increased.

The C_D of the airfoil and rotating cylinder remains identical up to 8° of angle of attack. The drag increases slightly on the rotating cylinder configuration due to the addition of cylinder.

TABLE III. COMPARISON OF AERODYNAMIC PERFORMANCE

ANGLE OF ATTACK	BARE AIRFOIL			AIRFOIL WITH STATIC CYLINDER			AIRFOIL WITH ROTATING CYLINDER		
	C_L	C_D	L/D	C_L	C_D	L/D	C_L	C_D	L/D
0°	0.204	0.0126	16.19	0.201	0.014	14.28	0.207	0.0127	16.299
4°	0.571	0.0151	37.80	0.515	0.0315	16.4	0.587	0.0147	39.93
8°	0.880	0.026	33.84	0.868	0.1458	5.953	0.974	0.0307	31.72
12°	1.080	0.054	20	0.521	0.1795	2.902	1.197	0.0783	15.28
16°	1.170	0.131	8.93	0.719	0.283	2.540	1.213	0.168	7.22

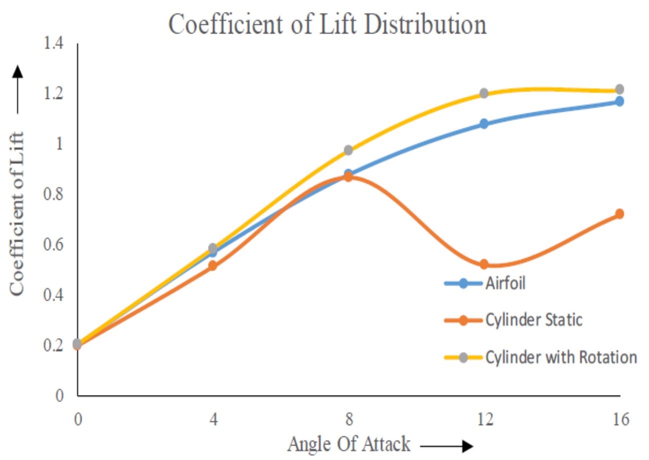

(a)

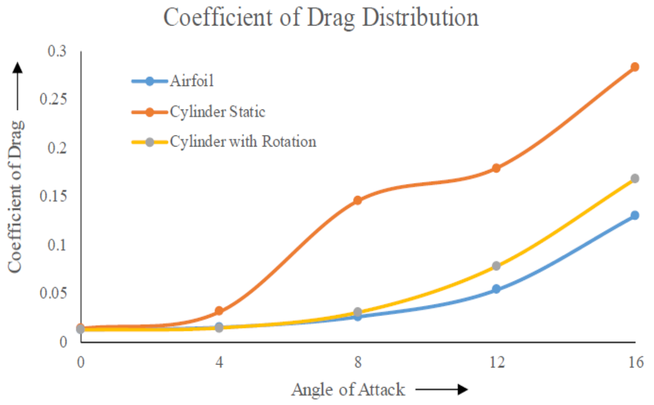

(b)

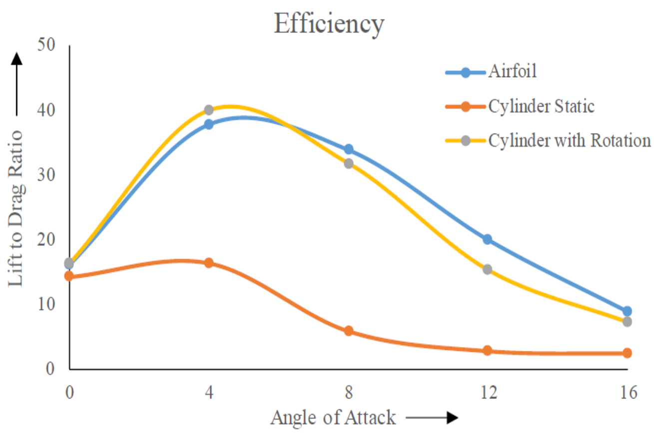

(c)

Fig 12. (a) Angle of Attack v/s Coefficient of Lift Distribution. (b) Angle of Attack v/s Coefficient of Drag Distribution. (c) Angle of Attack v/s Efficiency.

The static airfoil has the highest L/D ratio of 37.8 at an angle of attack of 4°, this is surpassed by the rotating cylinder configuration which has a maximum value of 39.93 at the same angle of attack. The static cylinder configuration has a very low L/D ratio, due to the cylinder rotation with an angular velocity of 11000rpm the L/D ratio increases by about 2.5 times.

The Lift coefficient of the static cylinder configuration drops rapidly after 8°. The Lift coefficient of the cylinder with rotation is slightly higher than the bare airfoil at all angles of attack. Therefore it is evident from the data obtained and tabulated that the rotating cylinder configuration enhances the lift producing capabilities of an airfoil at all angles of attack

A. Pressure contours

The pressure contours of the bare airfoil and rotating cylinder configuration at various angle of attack is shown in the following figures. The rpm is kept constant at 11000 for all angles of attack.

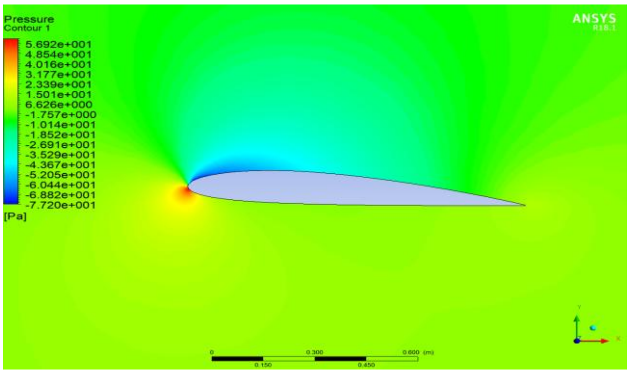

(a)

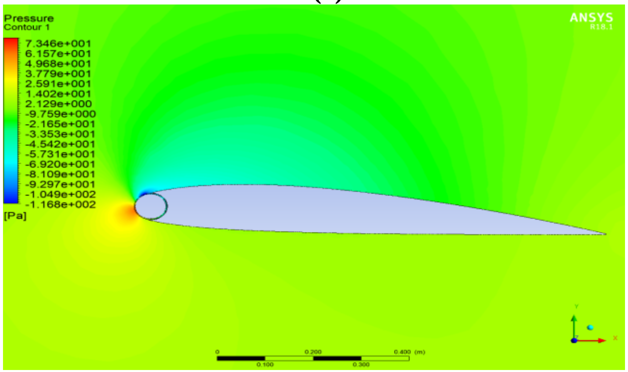

(b)

Fig 13. Pressure contours at 4° angle of attack (a) Bare airfoil. (b) Rotating cylinder

The pressure contours are compared between the airfoil and the rotating cylinder configuration at an angle of attack of 40. It is observed that there is a high pressure acting in front of the cylinder as compared with the airfoil, this is because the cylinder has a blunt shape at the leading edge. As the cylinder rotates the pressure at the suction side of that airfoil is lower as compared to the bare airfoil. This can explain the slight increase in the lift produced.

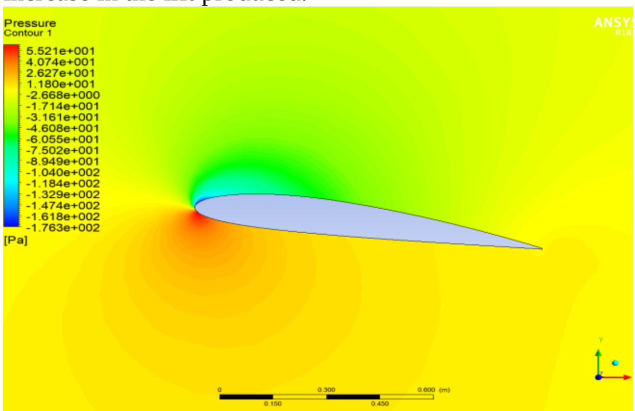

(a)

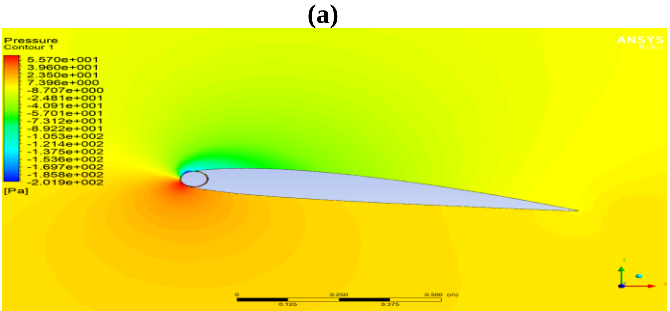

(b)

Fig 14. Pressure contours at 8° angle of attack (a) Bare airfoil. (b) Rotating cylinder

The pressure contours are compared between the airfoil and the rotating cylinder configuration at an angle of attack of 8°. The high pressure acting at the leading edge is similar in both cases but the low pressure values at the suction side is lower in the rotating cylinder configuration as compared to the bare airfoil.

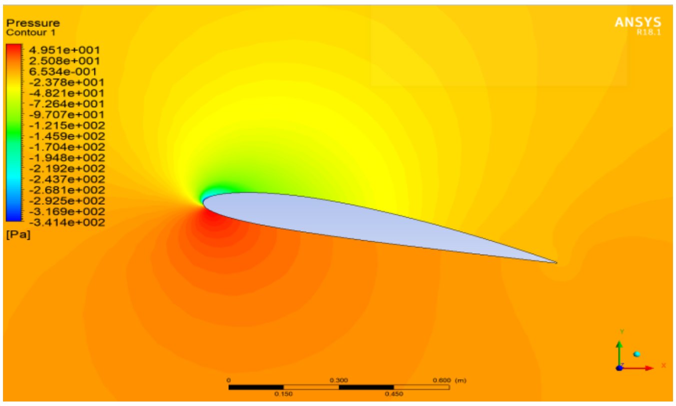

(a)

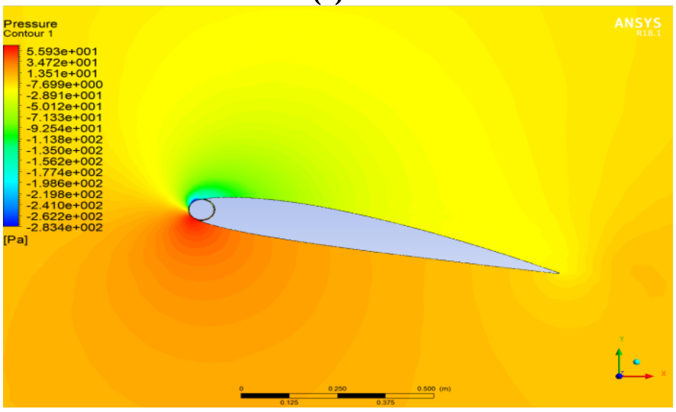

(b)

Fig 15. Pressure contours at 12° angle of attack (a) Bare airfoil. (b) Rotating cylinder

The pressure contours are compared between the airfoil and the rotating cylinder configuration at an angle of attack of 12°. The pressure difference between the pressure surface and suction surface is visibly higher in the rotating cylinder configuration when compared to the bare static airfoil. This explains the reduction in drag in the rotating cylinder configuration.

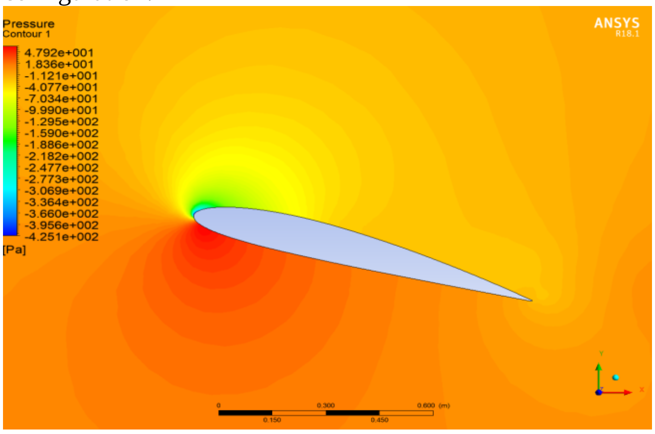

(a)

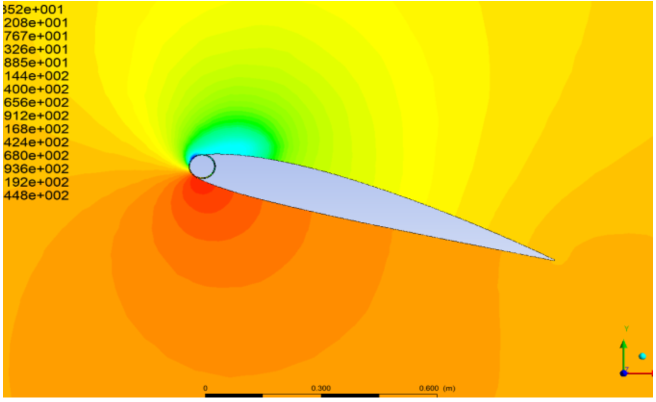

(b)

Fig 16. Pressure contours at 16° angle of attack (a) Bare airfoil. (b) Rotating cylinder

The pressure contours are compared between the airfoil and the rotating cylinder configuration at an angle of attack of 16°. The pressure at the leading edge is significantly higher in the rotating cylinder configuration compared to bare static airfoil, this can explain the significant reduction in drag compared to static cylinder configuration.

B. Velocity Contours

The velocity contours of the bare airfoil and rotating cylinder helps in understanding the flow separation point and drag over the surface. The following figures shows the configuration at different angle of attack. The speed of the rotating cylinder is 11000rpm.

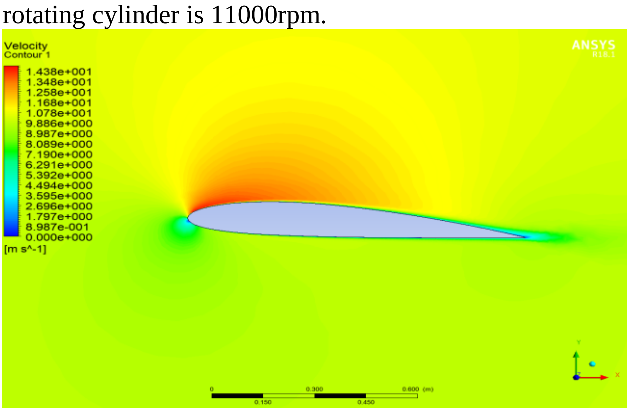

(a)

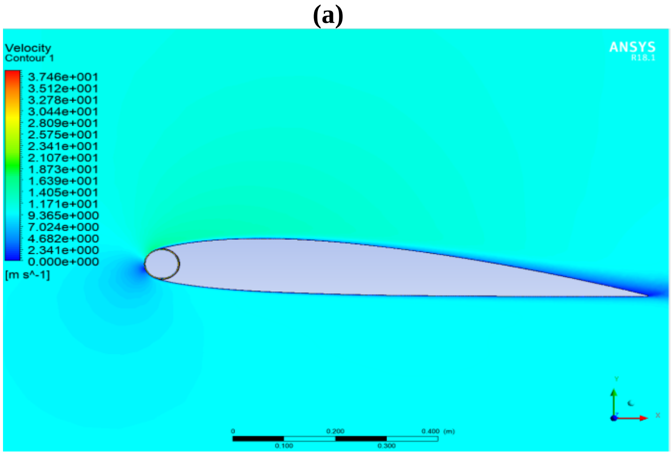

(b)

Fig 17. Velocity contours at 4° angle of attack (a) Bare airfoil. (b) Rotating cylinder

The velocity contours are compared between the airfoil and the rotating cylinder configuration at an angle of attack of 4°. The significantly higher velocity in Fig 17(b) is due to the fact that cylinder rotation causes a high velocity in the clearance between the cylinder and at the airfoil, due to the shape of the cylinder at the leading edge the velocity downstream is lower than the airfoil, but when the cylinder rotates with an angular speed, the velocity on the suction side is increased.

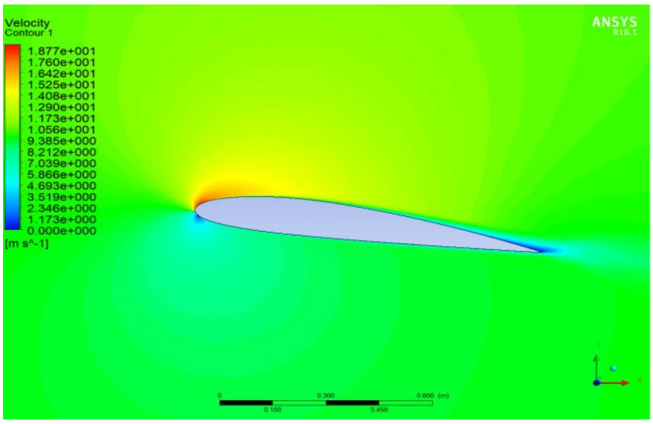

(a)

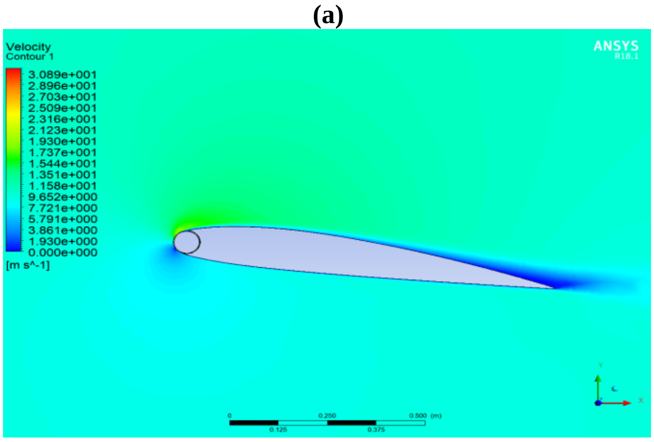

(b)

Fig 18. Velocity contours at 8° angle of attack (a) Bare airfoil. (b) Rotating cylinder

The velocity contours are compared between the airfoil and the rotating cylinder configuration at an angle of attack of 8°. The flow around the upper surface of the cylinder is smoother when compared to the bare airfoil but near the trailing edge, the flow velocity of rotating cylinder configuration is lower compared to the bare airfoil.

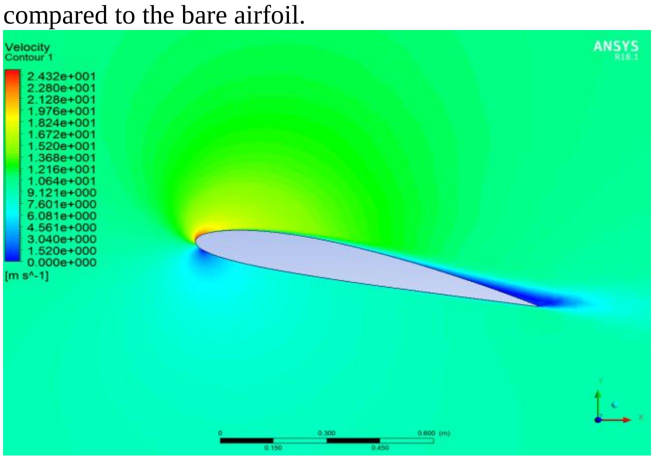

(a)

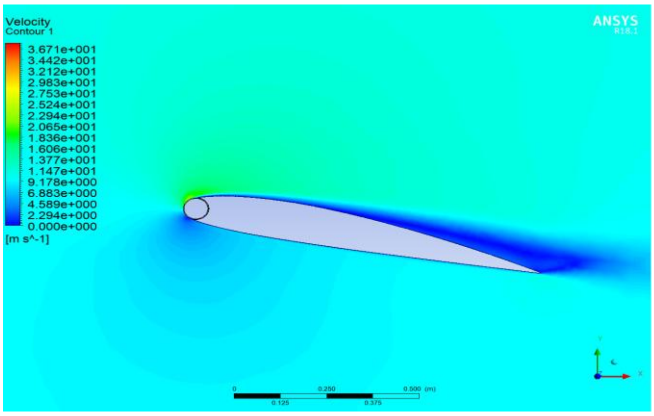

(b)

Fig 19. Velocity contours at 12° angle of attack (a) Bare airfoil. (b) Rotating cylinder

The velocity contours are compared between the airfoil and the rotating cylinder configuration at an angle of attack of 12°. The rotating cylinder configuration has higher velocity at the leading edge but deteriorates towards the trailing edge when compared to the bare airfoil.

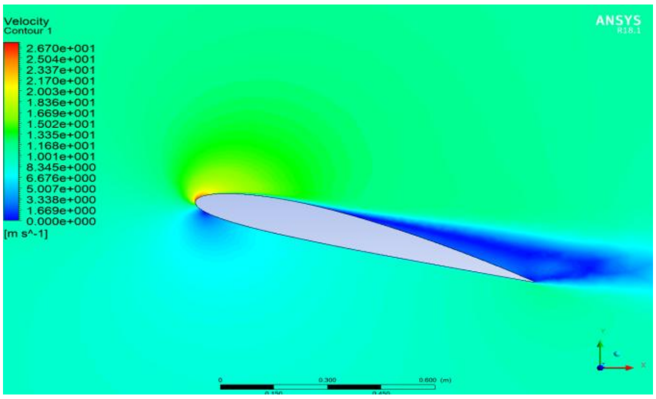

(a)

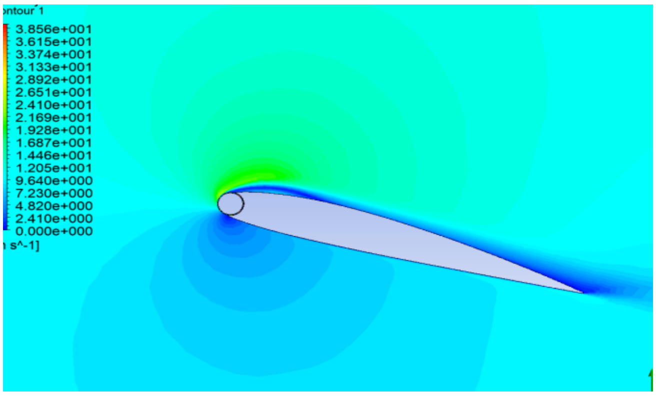

(b)

Fig 20. Velocity contours at 16° angle of attack (a) Bare airfoil. (b) Rotating cylinder

This velocity contour shows the airfoil stalling, the lift coefficient decreases with a further increase with angle of attack. In fig 20(b), the wake starts forming on the suction surface of the airfoil, this occurs because the slit of the configuration becomes tangential to inlet velocity, thereby increasing drag.

IV. CONCLUSION

The concept of energizing and controlling of the boundary layer is understood by employing a rotating cylinder at the leading edge of the cambered NACA 2412 airfoil. The boundary layer on the suction surface gets energized by the action of rotating cylinder and potentially delaying the stall and boundary layer separation. The CFD analysis gave us the insight on how a rotating cylinder energizes the boundary layer and increases the aerodynamic performance. From the above results we observe an increase in the lift coefficient and thereby an increase in the efficiency of the airfoil. Further this analysis can be improved by employing blades of different shape and size to increase the performance. This has a potential employing as a high lift device. In conclusion the rotating cylinder produces improved lift, thereby potentially increasing take-off performance or whenever an increased lift is required.

REFERENCES

1. ER. Shivam Saxena, Mr. Rahul Kumar, “Design of NACA 2412 and its analysis at different angle of attacks, Reynolds number and a wind tunnel” .
2. M Lopes,D. Welsh, R. Gates, J. Hoover, Mr. Lester, “The effects of a leading edge rotating cylinder on the performance of a NACA 0015 airfoil at high angles of attack”.
3. Ahmed Z. Al-Ghani, Abdullah M. Al-Ghani, Saad A. Ahmed, Ahmet Z. Sahin,” Flow control over an airfoil with leading edge rotation”.
4. Dr. John E Matsson, John A. Voth, Mr. Connor A. McCain, Mr. Connor McGraw,” Aerodynamic performance of the NACA 2412 airfoil at low Reynold’s number”.
5. F. Finaish, R. Jefferies,”Influence of rotating leading edge on accelerating starting flow over an airfoil”.
6. Argin Nazar,” Control of flow past an airfoil section using rotating cylinder”.
7. Najdat Nashad Abdulla, Mustafa Falih Hasan,” Effect of gap between airfoil and embedded rotating cylinder on the airfoil aerodynamic performance”.
8. Abhishek Sharma, Tejas Mishra, Sonia Chalia, Manish K. Bharti,” Subsonic flow analysis on rotating cylinder airfoil”.
9. X. Du, T. Lee, F. Kafyeke F Mokhtarian,” Flow past an airfoil with leading edge rotation cylinder”
10. V. Modi, F. Mokhtarian, M. Fernando,” Moving surface boundary layer control applied to two-dimensional airfoils”.
11. John D Anderson Jr, “Fundamentals of aerodynamics” India, McGraw Hill education, 2016.

AUTHORS PROFILE

Dharmendra A Ponnaswami, Assistant Professor at Dayananda Sagar College of Engineering. His qualifications are Bachelor of Engineering in Mechanical Engineering and Master of Technology in Aeronautical Engineering. He has presented a paper on “Study on Advanced Materials for Aircraft Jet Engines” ICCSEM-2013. He has been the technical support and faculty coordinator member of Institute of Aeronautics, Astronautics and Aviation (IAAA) since 2017 and also professional member of Institute of Engineering Research and Publication (IFERP) since 17th Dec 2019. He also has given a conference on the title “ Static aero-elastic analysis of wind tunnel test model in transonic flow” AIP conference proceedings 2204, 030006 (2020).

Abhinav Verma 8th semester student studying Bachelor of Engineering in Aeronautical Engineering. His area of interest include Reusable Launch Systems, Aerodynamics, Spacecraft propulsion Systems. He's a member of Aeronautical Society of India. He has worked on Flow Visualization over a Moto GP helmet and various CFD project

Chandana J P Reddy, 8^{th} semester student studying Bachelor of Engineering in Aeronautical Engineering. Her area of interest includes Avionics, Aircraft Propulsion. She's a member of the Aeronautical Society of India.

Jitvan Suri S, 8^{th} semester student studying Bachelor of Engineering in Aeronautical Engineering. His area of interest include Avionics, Aerodynamics, Hybrid Technologies. He's a member of Aeronautical Society of India. He has worked on rudder optimization CFD project.

Vishal M, 8^{th} semester student studying Bachelor of Engineering in Aeronautical Engineering. His area of interest include Aerodynamics, UAV design and Structures. He's been part of SAE Aero Design which was placed 8^{th} rank overall worldwide. He's member of Aeronautical Society of India. He has worked on critical Mach number CFD project and various project in CFD.